Transient Numerical Models of Metal Cutting using the Johnson-Cook's Rupture Criterion.

Jean-Louis Bacaria, Olivier Dalverny, Olivier Pantalé, Roger Rakotomalala

Transient Numerical Models of Metal Cutting using the Johnson-Cook's Rupture Criterion

Jean-Louis Bacaria — Olivier Dalverny — Olivier Pantalé
Roger Rakotomalala

Laboratoire Génie de Production, Equipe C.M.A.O.
Ecole Nationale d'Ingénieurs de Tarbes (ENIT)
Avenue d'Azereix
B.P. 1629
F-65016 Tarbes Cedex
roger@enit.fr

ABSTRACT. *This paper presents two-dimensional and three-dimensional transient numerical models of metal cutting. The simulations concern the study of the unsteady process of chip formation. These finite element models take into account dynamic effects, thermo-mechanical coupling with a rupture criterion and contact with friction. The yield stress takes into account the strain, the strain rate and the temperature in order to reflect realistic behavior in metal cutting. The rupture criterion adopted in the models presented here allows the definition of advanced simulations of the tool's penetration into the workpiece and of chip formation. The originality of such a criterion is that it is applied on all the workpiece and enables complex tool trajectories. Stress and temperature distributions, chip formation and tool forces are shown at different stages of the cutting process.*

KEYWORDS: *Metal Cutting, Turning, Milling, Rupture Criterion, Finite Element Model.*

1. Introduction

The development of a machining process requires considerable investment of time and resources. Process features such as tool geometry and cutting speed directly influence chip morphology, cutting forces, the final product dimensionality and tool life. Computer simulations of the cutting process can reduce the number of design iterations and results in cost savings. Considerable effort has therefore been devoted to the development of computational models for high speed machining.

Numerical models appeared at the beginning of the seventies; Eulerian models [IWA 84, CAR 88] and many Lagrangian models [CHI 90, SEK 92, LIN 92], have been developed for the simulation of metal cutting. Generally, these models provide information about stresses and strain fields, shear zones, and temperature fields. In 1985, Strenkowski and Caroll [STR 85] presented a thermo-mechanical model which predicted residual stresses in the workpiece, like Shih *et al.* [SHI 90] in 1990. Lin and Pan [LIN 93], have studied tool forces and have compared the results with experiments. Sekhon et Chenot [SEK 93] in 1993, also showed tool forces and stress distributions. Other well-known authors such as Marusich and Ortiz [MAR 95], Fourment *et al.* [FOU 97], Obikawa *et al.* [OBI 97] have developed unsteady models applied to metal cutting. The difficulty with this kind of model is in determining the method allowing element and node separation, and thus chip formation. All of us have used a criterion to realize this operation. A critical distance is used by [SHI 90], between the tip of the cutting tool and the nodal point located immediately ahead. Obikawa *et al.* [OBI 97] have presented a model with a double-criterion based on the value of a critical plastic strain and a geometric criterion for the simulation of fragmented chip formation. Other models use a critical plastic strain [STR 85] or the strain energy density [LIN 92] to allow separation. These criteria are generally arbitrary and are predefined on a nodal line which is followed by the face of the cutting tool. Most of them give good results close to the real cutting behavior but the use of such criteria limit simulations, they could not simulate complex tool trajectories as in the milling operation example. The use of separation criterion depending on each material, determined experimentally and applied to the whole material would give a better representation of reality. This is the method which we are going to develop.

In this paper, a two-dimensional and a three-dimensional finite element model of turning are presented. These models simulate the formation of continuous and discontinuous chips during the process according to the material machined (ductile or brittle). The results are compared with other existing numerical models and with experiments. An extension to a three dimensional finite element milling model is also described to illustrate complex tool trajectories and to show the possibilities of the use of the rupture criterion. The rupture criterion adopted here allows advanced simulations of the tool's penetration and chip formation. This rupture criterion was first initiated by Hancock and Mackenzie [HAN 76] and later developed by Johnson and Cook [JOH 85]. It needs the determination of five constants from tensile and

torsion tests which must be determined for each material used for the simulation. Its main advantage is avoiding the use of the classical predefined failure line.

Dynamic effects, thermomechanical coupling, rupture criterion and contact friction are taken into account. The yield stress takes into account the strain, the strain rate and the temperature. To reduce numerical problems for these simulations, an Arbitrary Lagrangian Eulerian formulation (ALE) has been adopted; already used by Rakotomala *et al.* [RAK 93], Pantalé [PAN 96] and Joyot [JOY 94].

2. Finite element discretization

An Arbitrary Lagrangian Eulerian formulation (ALE) is used for these simulations; this approach combines the advantages of both Eulerian and Lagrangian representations in a single description, and is exploited to reduce finite element mesh distortions, [RAK 93, JOY 94, PAN 96]. Numerical simulations are realized on ABAQUS V.5.8.

2.1. *Conservation laws in ALE description*

The equations which govern the continuum in the ALE description are the three conservation laws. In view of spatial discretization of the mass, momentum and energy equations by the finite element method, a classic variational form is obtained by multiplying these equations by a weighting function ($\overset{*}{\rho}$, $\overset{*}{v_i}$, $\overset{*}{e}$) over the spatial domain R_χ. Employing the divergence theorem, the variational forms associated with these equations are given by:

$$\int_{R_x} \overset{*}{\rho} \overset{\circ}{\rho} dR_x + \int_{R_x} \overset{*}{\rho} c_i \rho_{,i} dR_x + \int_{R_x} \overset{*}{\rho} \rho v_{i,i} dR_x = 0 \qquad [1]$$

$$\int_{R_x} \rho \overset{*}{v_i} \overset{\circ}{v_i} dR_x + \int_{R_x} \rho \overset{*}{v_i} c_j v_{i,j} dR_x = -\int_{R_x} \overset{*}{v}_{i,j} \tau_{ij} dR_x + \int_{R_x} \overset{*}{v_i} f_i dR_x + \int_{\Gamma_x} \overset{*}{v_i} h_i d\Gamma_x \qquad [2]$$

$$\int_{R_x} \rho \overset{*}{e} \overset{\circ}{e} dR_x + \int_{R_x} \rho \overset{*}{e} c_i e_{,i} dR_x = \int_{R_x} \overset{*}{e} \sigma_{ij} v_{(i,j)} dR_x \qquad [3]$$

In these expressions, $\overset{\circ}{()}$ is the nodal rate variation, ρ is the mass density, v_i the material velocity, h_i the surface force, f_i the body forces, τ_{ij} the Cauchy stress tensor, e the internal energy, $v_{(i,j)}$ the strain rate tensor. $c_i = v_i - w_i$ is the

relative velocity between the material velocity (v_i) and the mesh velocity (w_i). The model is adiabatic and the temperature calculated in the workpiece is only du to plastic deformations.

Quadrilateral elements with four nodes and a reduced integration point have been used to generate these simulations. Zero energy modes are generated by Hourglass control for the momentum equation, and the transport terms are generated by an Upwind procedure.

2.2. *Explicit dynamic analysis*

The equations of motion for the body are integrated using the explicit central difference integration rule.

$$v^{(i+1/2)} = v^{(i-1/2)} + \frac{\Delta t^{(i+1)} + \Delta t^{i}}{} \dot{v}^{(i)} \qquad [4]$$

where v is the velocity and $\dot{v}$ the acceleration. The superscript (i) refers to the increment number, (i-1/2) and (i+1/2) refer to the midincrement values. The central difference integration operator is explicit in that the kinematic state can be advanced using known values of $v^{(i-1/2)}$ and $\dot{v}^{(i)}$ from the previous increment. The explicit procedure integrates through time by using many small time increments. A stable time increment is computed for each element in the mesh.

3. Material and contact laws

The material law of the original Johnson-Cook [JOH 83] form is used for the simulations presented in this paper. This relationship is frequently adopted for dynamic problems with high strain rates and temperature effects.

Assuming a Von Mises type yield criterion and an isotropic strain hardening rule, the flow rule is given by:

$$\sigma=(A+B\bar{\varepsilon}^{n})(1+C\ln\dot{\bar{\varepsilon}}^{*})(1-T^{*m}) \qquad [5]$$

where ε represents the equivalent plastic strain, $\dot{\bar{\varepsilon}}^{*} = \frac{\varepsilon}{\dot{\varepsilon}_0}$ the non dimensional equivalent strain rate and $T^{*} = (T - T_0)/(T_{melt} - T_0)$ depends on temperature. T_0 is the initial temperature and T_{melt} the melting temperature. $\dot{\varepsilon}_0$ the equivalent strain rate material reference value at which the material begins to be sensitive to this

effect. A , B , C , n and m are material parameters, and are given by Johnson and Cook [JOH 83] for a 4140 steel, corresponding to a 42CD4 steel (French standard). The values of the material constants are obtained from torsion tests (over a wide range of strain rates), static tensile tests, dynamic Hopkinson bar tensile tests and Hopkinson bar tests at elevated temperatures.

Many models of friction applied to cutting process exist in the literature as the laws of Kato or Montgomery [KAT 72, MON 76]. However the aim of this paper is the study of the influence of a rupture criterion on a numerical model of metal cutting. For this reason, we have chosen to modelise the tool-chip interface with the simple Coulomb friction law. With this model, we assume and the stick/slip condition is given by:

$$\text{Slip if } |T^t| \geq C_f\,|T^n|, \text{ stick if } T^t| < C_f\,|T^n| \qquad [6]$$

in which C_f is the coefficient of friction; T^n and T^t are, respectively, the normal and tangential components of the surface traction on the interface.

4. Rupture criterion

The use of a rupture criterion (or chip criterion), was of prime necessity in modeling a realistic tool penetration phase during the unsteady metal cutting simulation, although the arbitrary chip criterion commonly used for these studies presupposes the progress of the crack zone [STR 85, LIN 92, SHI 90]. In opposition, our rupture criterion is able to show the rupture state of the materials according to the local thermo-mechanical load applied.

This rupture criterion D was first developed by Hancock and Mackenzie [HAN 76] and later by G. R. Johnson and W. H. Cook [JOH 85]. It is defined to simulate ductile failure with high strain, strain-rate and temperature effects. The total rupture for each element is calculated using the relationship given below:

$$D = \sum \frac{\Delta \bar{\varepsilon}}{\bar{\varepsilon}^f} \qquad [7]$$

where $\Delta \bar{\varepsilon}$ is the increment of equivalent plastic strain which occurs during an integration cycle, and $\bar{\varepsilon}^f$ is the equivalent strain to failure under the current conditions. Fracture is allowed to happen when $D = 1$ and thus the concerned elements are removed from the mesh. The strain at fracture is given by :

$$\bar{\varepsilon}^f = \left[D_1 + D_2 \exp D_3 \sigma^*\right]\left[1 + D_4 \ln \dot{\varepsilon}^*\right]\left[1 + D_5 T^*\right] \qquad [8]$$

depending on the variables (σ^* , $\dot{\varepsilon}^*$, T^*). The dimensionless pressure-stress ratio is defined as $\sigma^* = \sigma_m / \sigma$ where σ_m is the average of the three normal stresses and $\overline{\sigma}$ the Von Mises equivalent stress. The dimensionless strain rate $\dot{\varepsilon}^*$, and homologous temperature T^*, are identical to those used in the material constitutive law previously defined.

The expression in the first set of brackets of equation [8] follows the form presented by J.W. Hancock and A.C. Mackenzie [HAN 76], and essentially indicates the decrease in strain fracture as the hydrostatic pressure (σ_m) increases and the yield stress decreases. The second set of brackets represents the effect of strain-rate, and the third set the temperature effects. These two sets of brackets could be neglected, as it is explained in the Johnson-Cook article, due to their low influence on the results. We have thus verified this point using metal cutting simulation, in which we have used the material parameters of Johnson and Cook for the 4340 steel [JOH 85]. The first simulation was made with a complete criterion (D_1, D_2, D_3, D_4, D_5) and the second with a limited criterion (D_1, D_2, D_3). From the results, we noticed that the influence of D_4 and D_5 is insignificant in cutting context. For this reason and according to the Johnson-Cook works [JOH 85], we neglect the strain rate and temperature effects (*i.e.* D_4 and D_5).

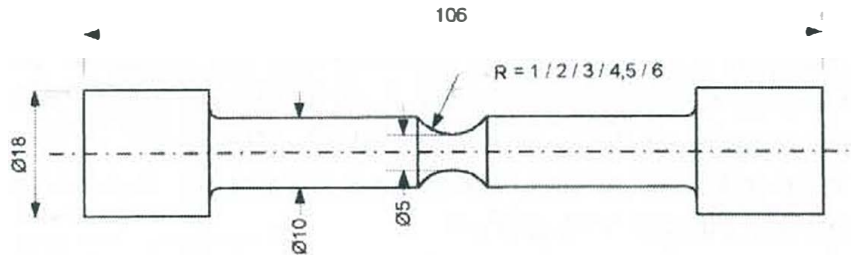

Figure 1. *Tensile test specimens*

The constants of the Johnson/Cook rupture criterion D_1, D_2, D_3,, are identified from tensile tests [JOH 85]. The values are different depending on the material tested. According to the bibliography, these parameters are known only for three materials (copper, iron and 4340 steel) but not for 4140 steel which is the material used for our simulations and experimental validations. Thus it was necessary to carry out tensile tests to determine D_1, D_2, and D_3, for the 4140 steel following the procedure [JOH 85]. The tensile tests were carried out in our laboratory on a tensile test machine with notched specimens with different radius curvatures (Figure 1).

CCD cameras (Figure 2) and the Aramis 3D (Figure 3) system have also been used to measure displacement fields in the cracked zone and to deduce strain fields.

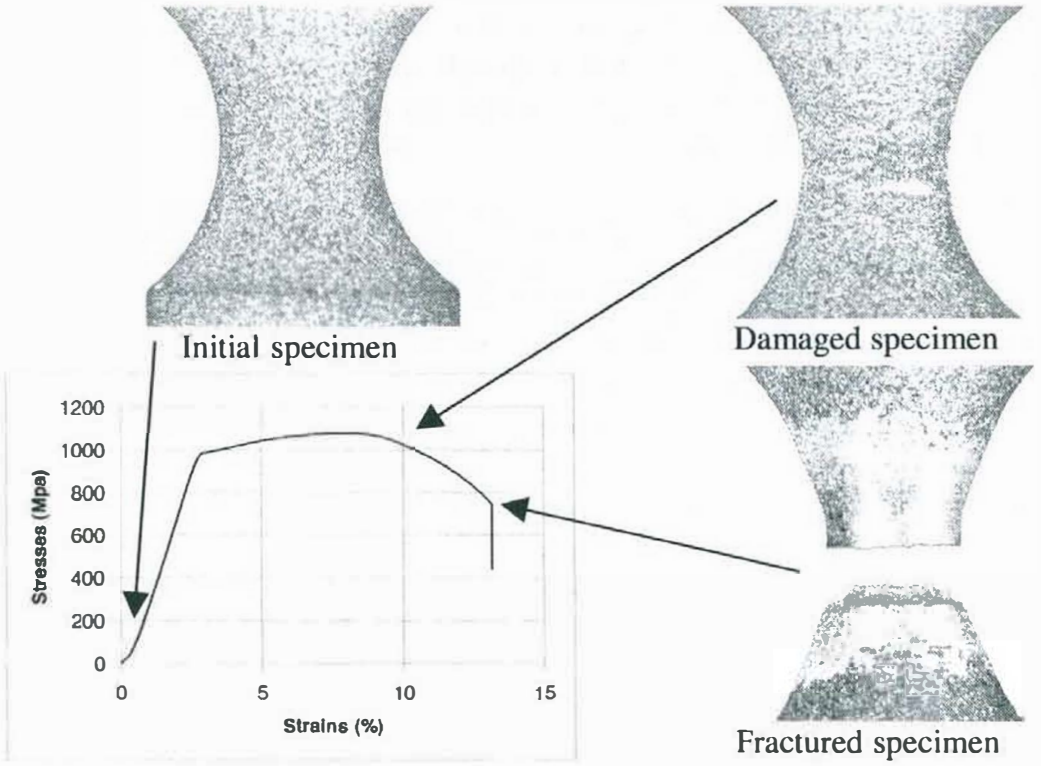

Figure 2. *CCD pictures at different steps of the tensile test*

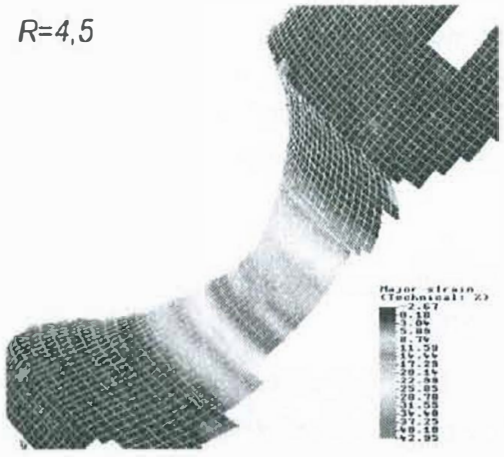

Figure 3. *Strain fields for a specimen with a radius curvature of R = 4.5 mm*

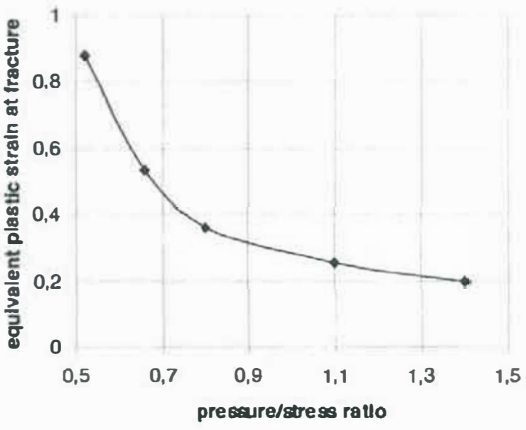

Figure 4. *Results of the 4140 steel*

The measurements obtained, after the tensile test of each specimen, enable the determination of the equivalent plastic strain at rupture. Pairs of values obtained ($\sigma^*, \bar{\varepsilon}^J$) are shown in the graph, (Figure 4). To determine the three material

parameters D we have used a program to minimize the response error between the curve and experimental results. The values of the constants for the 4140 steel are: $D_1 = 1.5$, $D_2 = 3.44$ and $D_3 = -2.12$. This steel will now be used for the metal cutting simulations. The rupture criterion is defined for the 4140 steel and could be taken into account in the numerical models.

5. Numerical model of turning

The application of this rupture criterion has been carried out using the turning operation. The results are presented for a two and a three dimensional simulation of orthogonal metal cutting. In these unsteady models of chip formation, the tool is considered to be rigid, and to move at a constant cutting velocity of 4m/s (Vc) with a cutting depth of 0.5 mm (a) and a depth width of 2 mm. The workpiece is fixed on its base and only the tool is free to move. The material used is a low alloy 4140 steel. The rigid cutting tool has a rake angle and a relief angle equal to 5.7° and the radius of the cutting edge is equal to 0.1mm. The initial temperature of the workpiece is assumed to be 300 K. The friction coefficient between the tool and the chip is modeled with Coulomb law and is equal to 0.32 (C_f). This value was obtained on an experimental basis applying a normal force to the tool in contact with the moving workpiece and by measuring the corresponding tangential forces. The rupture criterion is applied to the whole workpiece.

The material parameters for the 4140 steel are presented below:

$E = 210GPa$, $\upsilon = 0.3$

$A = 595MPa, B = 580MPa, C = 0.023$, $m = 1.03$, $n = 0.133$

$D_1 = 1.5, D_2 = 3.44, D_3 = -2.12$

$C_p = 379J/kgK$, $\rho = 7800kg/m^3$

$T_{melt} = 1793K$

Classical quadrilateral elements with reduced integration are used. The initial mesh and the initial configuration are shown on Figure 5.

The first step of the simulation correspond to the analyze of the penetration of the tool into the workpiece. The second step is the analysis of the continuous chip formation and the comparison of the results between the two-dimensional and the three-dimensional models.

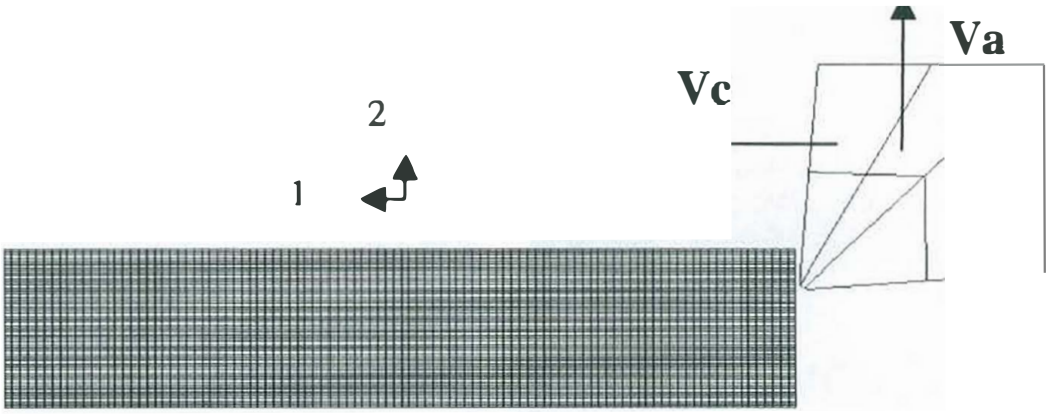

Figure 5. *Initial mesh of the two-dimensional turning model*

6. Results of the turning models

6.1. *Tool penetration*

The simulation shows tool penetration in the workpiece and chip formation (Figures 6a-6d). In the first step, the tool penetrates the workpiece and produces high compression on the tool rake face (Figure 6a). In the next step, rupture occurs at the nose of the tool which generates element separation and allows the material to flow along the tool face (Figure 6b). The primary shear band begins to appear with the decrease of compression on the tool face; the material continues to rise (Figure 6c). Finally, the primary shear band is created and the chip rises (Figure 6d). A decrease of Von Mises stress at the tool nose can be noted (Figures 6b-6d), due to the fact that the model eliminates ruptured elements.

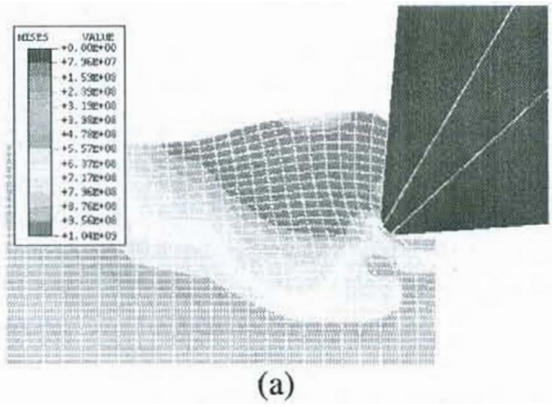

(a)

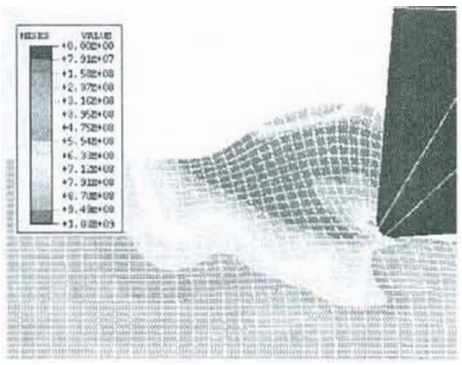

(b)

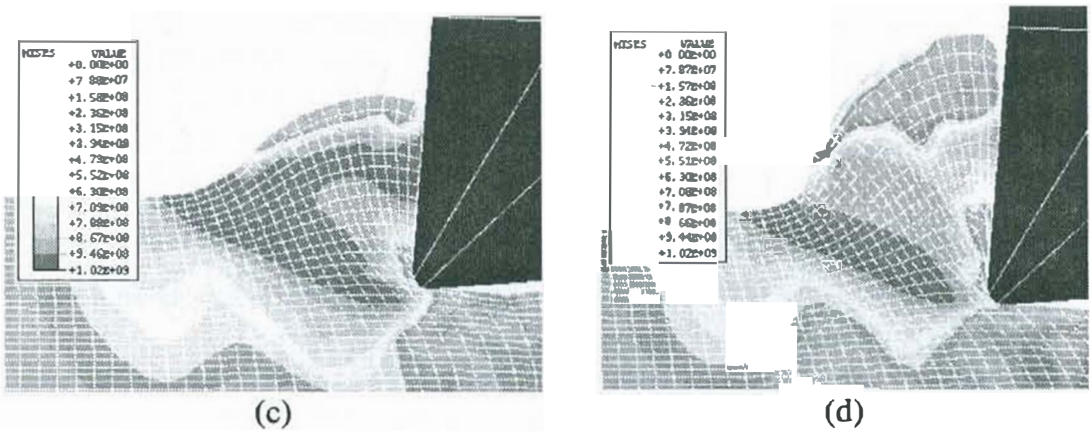

Figure 6. *Von Mises stresses and chip formation at different stages of simulation: (a) 0.08 ms; (b) 0.17 ms; (c) 0.26 ms; (d) 0.4 ms*

6.2. *Continuous chip formation*

The tool continues to progress into the workpiece, the material rises along the face of the tool and forms a continuous chip. The chip is continuous due to the material and cutting conditions used. The maximum Von Mises stress appears on the primary shear band, (Figure 7a). Temperature distribution, (Figure 7b), shows the maximum value at contact between the tool and the chip and on the machined surface. These results are in agreement with experiment observations and with other numerical models [JOY 94, PAN 96]. The comparison of the maximum Von Mises stress and the maximum temperature with other numerical models are presented in Table 1.

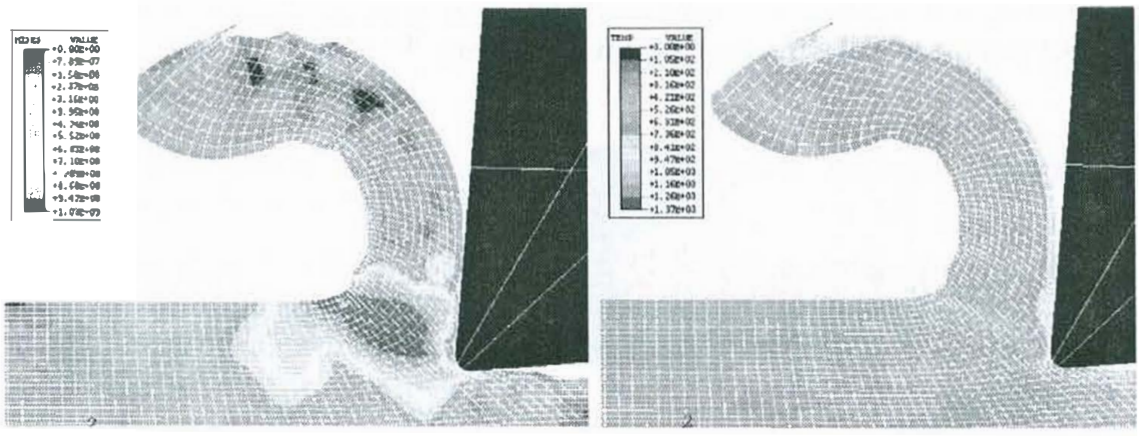

Figure 7. *Von Mises stress distribution (a) and temperature distribution (b)*

The validation of a metal cutting model is usually carried out by comparison of the cutting force with experiments. The cutting forces, *F1* and *F2*, (Figure 8)

obtained during the simulation are the projections respectively on direction 1 and 2 of the total cutting force. The primary oscillations (t = 0ms to t = 0.6ms) are due to the tool impact and chip formation. After this short period of oscillations, the principal cutting force (*F1*) is globally stabilized with a value of about 1800N. This is this cutting force which is usually compared with experiments for the validation of the cutting model.

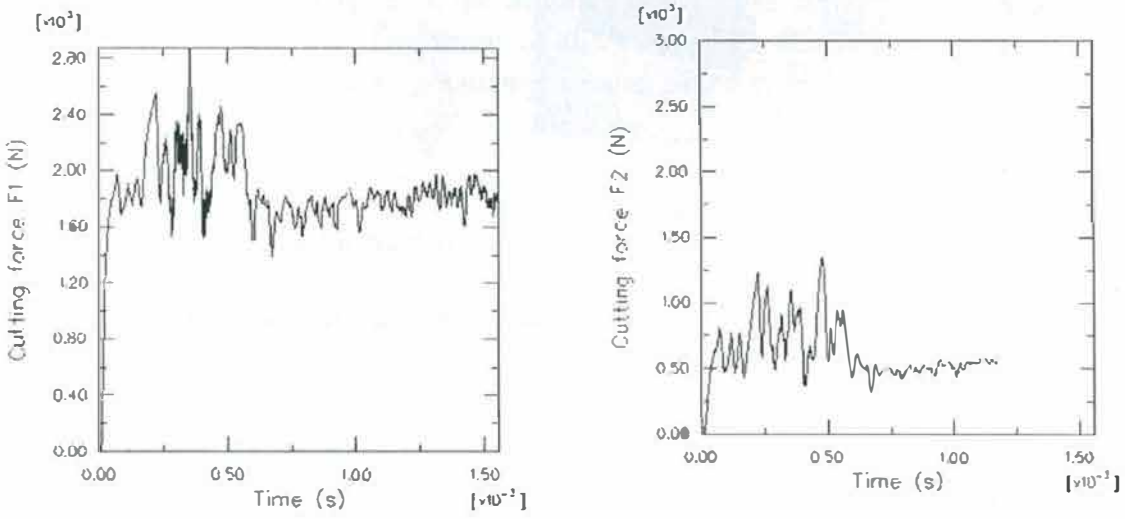

Figure 8. *Cutting force evolution versus time*

This is in agreement with bibliographic simulations and experiments performed with the same material and cutting conditions [JOY 94, PAN 96] (Table 1). It can be noted that the oscillations of the cutting force around the average value (after oscillations) depends on the refinement of the mesh coupled with the deletion of the damaged elements.

More investigations have recently been carried out using three-dimensional models of the cutting process. The first was by Maekawa *et al.* in 1990 [MAE 90] who simulated unsteady process of oblique chip formation. Ueda and Manabe [UED 93] have also developed a three-dimensional oblique model of unsteady chip formation. The chip separation criterion is based on geometrical consideration of the tool edge and work material. They have studied chip formation and cutting forces in function of inclination angle variation and have compared results with experiments. Original numerical and experimental studies were presented in 1994 by Sasahara *et al.* [SAS 94], in which nodes separate in function of critical distance coupled with critical equivalent plastic strain. The most recent model is due to Lin and Lin [LIN 99] who have presented a three-dimensional model, for continuous chip formation. The chip separation criterion used was based on the strain energy density also coupled with a critical distance.

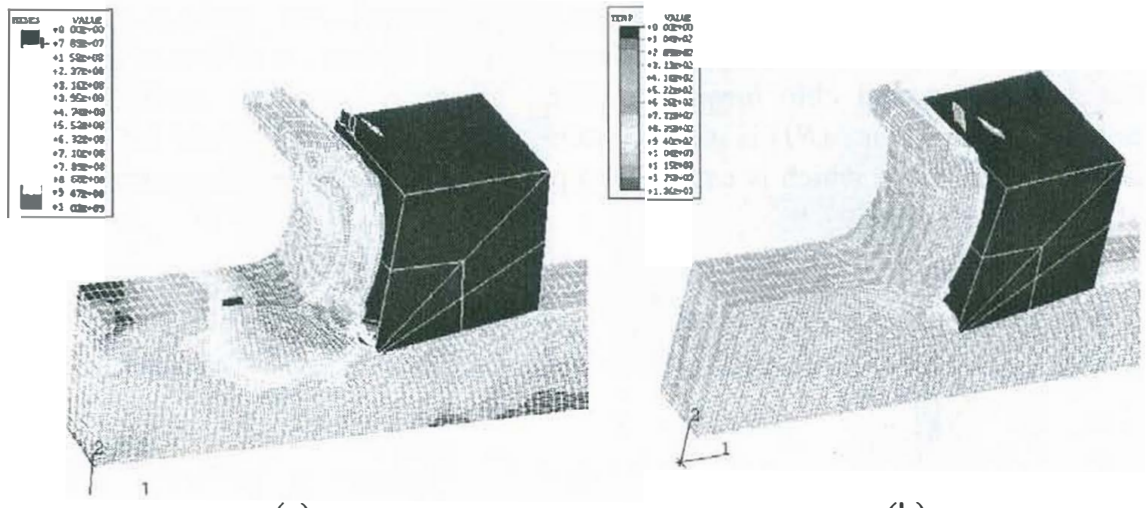

(a) (b)

Figure 9. *Von Mises stress distribution (a) and temperature distribution (b)*

To explore the possibilities of our rupture criterion we have also performed a transient three-dimensional model of continuous chip formation. This model simulates, like the two dimensional model, the tool penetration and the chip formation. It uses the same tool geometry and cutting parameters as the two-dimensional model. Material and rupture criterion are also the same. It can be noted that the tool is more wide than the workpiece to clearly put in evidence the side-effects which occur only in three dimensional simulation [PAN 96]. The blow-up of the chip at its base and the high temperature on the edges of the machined surface are characteristics of the side-effects. Von Mises stress and temperature distribution are shown in Figures 9a-b. We have also compared the maximum values of the Von Mises stress (σ_{max}) and the maximum temperature (T_{max}) with the results of the two-dimensional model (Table1).

Table 1. *Results comparison*

	Experiments	*Joyot*	*Pantalé*	*2D*	*3D*
σ_{max}		*1.4 GPa*	*1.0 GPa*	*1.03 GPa*	*1.03 GPa*
T_{max}		*1500 K*	*1400 K*	*1370 K*	*1360 K*
F_{1moy}	*1850 N*	*1740 N*	*2096 N*	*1750 N*	*1800 N*
F_{2moy}	*500 N*	*184 N*	*720 N*	*490 N*	*510 N*

In futures work, it would be interesting to study the force variation due to tool angle inclination (oblique cutting model).

The case of the continuous chip is interesting but has been developed many times in documented studies. The reasons are due to the stability of the process and the easy simulation of such a process with a classical chip criterion (the separation criterion defined along a straight line). The case of the fragmented chip formation is more complex to simulate because the fragmentation of the chip could not be carried out with such criteria. The definition of the node lines are too complex and the localization is unknown. It is necessary to use other criteria to simulate such a formation.

6.3. *Discontinuous chip formation*

The case of the discontinuous chip formation has however been studied analytically by Field and Merchant [FIE 49], Cook *et al.* [COO 54]. Marusich and Ortiz [MAR 95], Hashemi *et al.* [HAS 94], Obikawa *et al.* [OBI 97] have presented numerical models for discontinuous chip formation. Ortiz and Hashemi use crack propagation and their models give good results in comparison with experimental results. The Obikawa model uses a double criterion of separation. The first criterion is a critical distance which is applied to a line of node for the creation of the chip. The second is a fracture criterion (which allows chip fragmentation) expressed according to the strain, strain-rate, hydrostatic pressure and material parameters. The results show the influence of chip fragmentation on the cutting force evolution.

The advantage of using the rupture criterion defined earlier is the possibility of simulating continuous or discontinuous chip formation according to the material machined. The transient simulation example presented below is for the turning of a virtual brittle material and to illustrate such a case (Figure 10). The boundary conditions are the same on the workpiece as on the models defined earlier. Only the rupture of the material changes ($D_1 = 0.05, D_2 = 3.44, D_3 = -2.12$). This simulation presents results for a constant cutting depth of a=0.5mm and a cutting velocity Vc = 4m/s.

The maximum value of Von Mises stress occurs in the primary shear band as shown in Figure 10. The rupture occurs near the nose of the tool and propagates along the primary shear band to the surface of the chip in agreement with [COO 54]; in contrast to the continuous chip formation where the rupture propagates along a line in front of the tool nose. This case is a cyclic phenomenon which produces chip segmentation and thus discontinuous chip formation. The principal cutting force evolution (corresponding to the projection on direction 1) obtained on the tool during the process is shown in Figure 11. We can read clearly the chip segmentation on this graph, still in agreement with [COO 54] and [OBI 97]. This numerical model needs more investigation, but it shows one of the applications of the rupture criterion as an example.

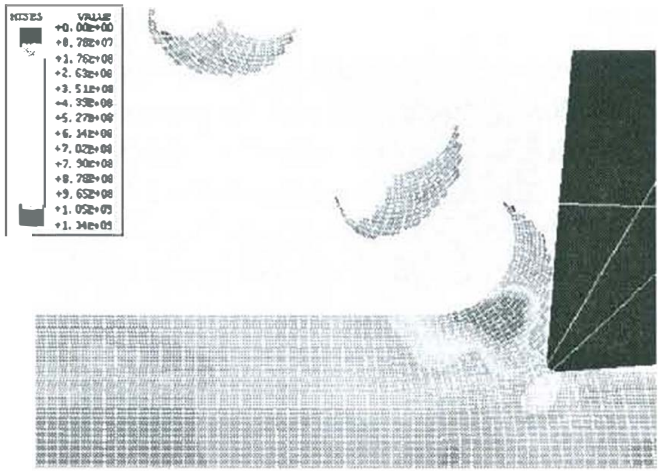

Figure 10. *Von Mises stress distribution*

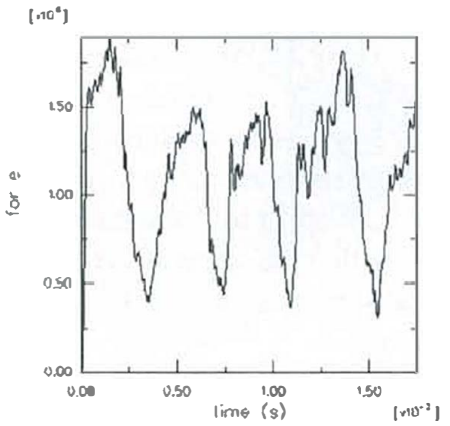

Figure 11. *Cutting force evolution*

Another interesting point of this rupture criterion is the possibility of defining arbitrary and complex tool trajectories. The tool trajectory is an important element in the definition of a numerical model of metal cutting; all models already developed are limited on this point due to their chip criteria. To illustrate such a case we have chosen to simulate a discontinuous chip formation with two velocities Vc=10m/s and Va = 0.5m/s. The initial cutting depth is equal to a = 0.5mm. The material machined is still the 4140 steel. The Von Mises stress distribution (Figure 12) shows a maximum value at about 1.0 GPa and two chips. When the simulation starts, the tool penetrates the workpiece as described earlier. The tool advances and when it arrives at a cutting depth of a = 0.1mm, the chip breaks into the primary shear band due to stress state. The breaking of the chip corresponds to the time t = 0.18ms on the cutting force evolution where the cutting force suddenly decreases (Figure 13).

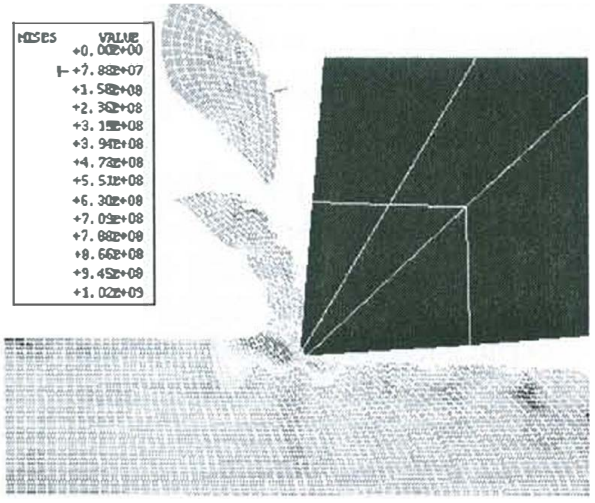

Figure 12. *Von Mises stress distribution*

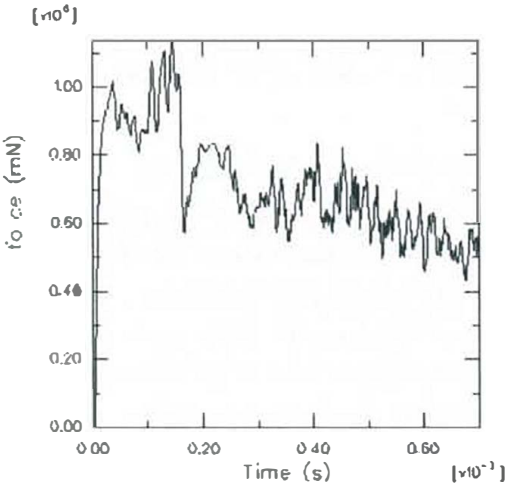

Figure 13. *Cutting force evolution*

The rest of the chip (which is not broken) is seriously damaged as we can see on the free surface and on the contact with the tool. The cutting force evolution, after the first chip, shows the decrease in magnitude due to the constant decrease in cutting depth. Usually numerical simulations of the cutting process present results on continuous or discontinuous chip formation. The simulation presented here corresponds to an intermediate configuration where the continuous or the discontinuous state directly depends on the cutting parameters like in reality.

To illustrate tool trajectories, it is known that the most complex case is certainly the milling operation and in our opinion it would be interesting to simulate such a process to determine what really the possibilities or the limits of the rupture criterion are.

7. Numerical model of milling

The use of such a rupture criterion avoids the problem of a predefined fracture line. The main advantage is to model complex tool trajectories and keep free chip formation. The case of a three dimensional milling simulation is so complex that is impossible to predict fracture node lines and it represents an interesting case for the testing of such a criterion.

The milling operation is presented using a three-dimensional simulation. The tool is considered to be rigid and to move at a rotating and a translating velocity. Only a part of a twist milling cutter has been modeled to reduce element number (Figure 14). The material used for the simulation is still the 4140 steel and the boundary conditions applied on the workpiece are the same as for the turning simulations. It seems that no such simulation has been developed yet, the main reason being the limits of the other criteria commonly used for metal cutting simulations. The results for one tooth which is in the middle of the simulation are presented. The initial mesh and initial configuration are shown in Figure 14.The results of the Von Mises stresses and chip formation are shown at two differents stages during the simulation (Figure 15).

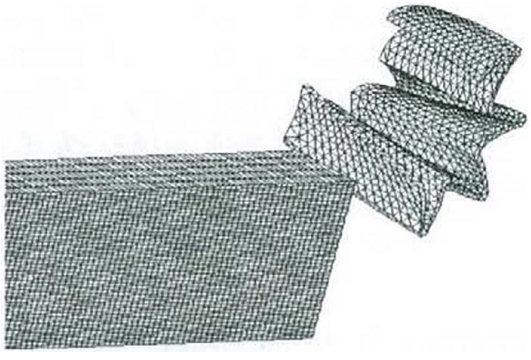

Figure 14. *Initial mesh and configuration*

When a tooth of the milling cutter penetrates the workpiece, the primary shear band is clearly visible (Figure 15a). At this time, the configuration is the same as for an oblique orthogonal metal cutting model. The chip is broken along the primary shear band due to the rotating velocity of the tool and the rupture of the material (Figure 15b). An instant later, the same tooth is out of the workpiece and a second tooth enters to cut the second chip. Only one tooth cuts the workpiece during the simulation; this is a cyclic phenomenon which produces segmented chips. The milling simulation could be compared to a cyclic oblique turning, and the twist milling cutter could be compared to a series of oblique tools. More investigation must be carried out in order to understand each step of the milling operation in studying shear bands and cutting forces.

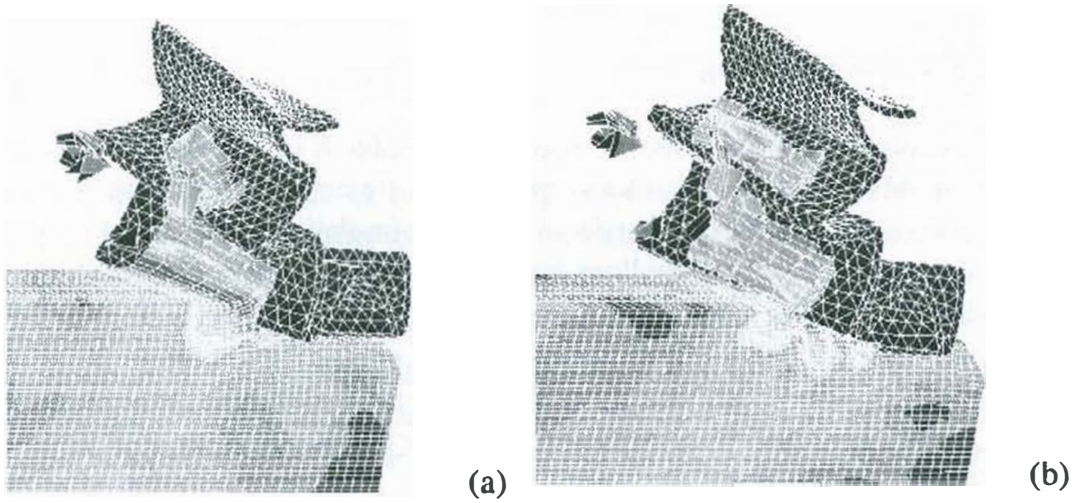

Figure 15. *Von Mises stress distribution for the milling simulation*

8. Conclusion

In this paper, transient cutting models for turning and milling metal have been presented. The results of the turning models are in agreement with other existing models and experiments. They take into account rupture due to tool penetration and chip formation. The material rupture criterion used permits realistic simulation. The comparisons with other experiments and models in the bibliography have confirmed that the Johnson-Cook rupture criterion gives good results for metal cutting behavior. Its main advantage is to avoid the classical predefined failure zone and to model cutting simulations for complex tool trajectories. More investigation will be carried out to exploit and validate the transient numerical model of milling.

9. References

[CAR 88] CARROLL J. T., STRENKOWSKI J., "Finite element models of orthogonal cutting with application to single point diamond turning", *Int. Journal. Mech. Sc.*, pp. 899-920, 1988.

[CHI 90] CHILDS T. H., MAEKAWA K., "Computer aided simulation and experimental studies of chip flow and tool wear in the turning of low alloy steels by cemented carbide tools", *Wear*, pp. 235-250, 1990.

[COO 54] COOK N. Y., FINNIE I., SHAW M. C., "Discontinuous chip formation", *Trans. ASME*, pp. 153-162, 1954.

[FIE 49] Field M., Merchant M. E., "Mechanics of formation of the discontinuous chip in metal cutting", *Trans. ASME*, pp. 421-430, 1949.

[FOU 97] FOURMENT L., OUDIN A., MASSONI E., BITTES G., LE CALVEZ C., "Numerical simulation of tool wear in orthogonal cutting", *1^er French and German Conference on High Speed Machining*, pp. 38-48, 1997.

[HAN 76] HANCOCK J. W., MACKENZIE A. C., "On the mechanisms of ductile failure in high strength steels subjected to multi-axial stress rates", *J. Mech. Phys. Solids*, pp. 147-149, 1976.

[HAS 94] HASHEMI J., TSENG A. A., CHOU P. C., "Finite element modeling of segmental chip formation in high speed orthogonal cutting", *Journal of Materials Eng. and Performance*, pp. 712-721, 1994.

[IWA 84] IWATA K., OSAKADA K., TERASAKA Y., "Process modeling of orthogonal cutting by the rigid plastic finite element method", *Journal of Engineering Materials and Technology*, pp. 132-138, 1984.

[JOH 83] JOHNSON G. R., COOK W. H., "A constitutive model and data for metals subjected to large strains, high strain rates and high temperatures", *Proc 7^th Inter. Symp. Ballistics*, pp. 541-547, 1983.

[JOH 85] JOHNSON G. R., COOK W. H., "Fracture characteristics of three metals subjected to various strains, strain rates, temperatures and pressures", *Eng. Fracture. Mech.*, pp. 31-48, 1985.

[JOY 94] JOYOT P., Modélisation numérique et expérimentale de l'enlèvement de matière, Thesis of Bordeaux University, France, 1994.

[KAT72] KATO S., YAMANDURI K., YAMADA M., "Stress distribution at the interface between tool and chip in machining", *Journal Eng. Industry*, pp. 683-689, 1972.

[LIN 92] LIN Z. C., LIN S. Y., "A coupled finite element model of thermo-elastic-plastic large deformation for orthogonal cutting", *Journal of Engineering Materials and Technology*, pp. 218-226, 1992.

[LIN 93] LIN Z. C., PAN W. C., "A thermoelastic-plastic large deformation model for orthogonal cutting with tool flank wear-part II", *Inter. J. Mech. Sci.*, pp. 841-850, 1993.

[LIN 99] LIN Z.C., LIN S.Y., "Fundamental modeling for oblique cutting by thermo-elastic-plastic FEM", *Inter. J. of Mechanical Sc.*, pp. 941-965, 1999.

[MAE 90] MAEKAWA K., NAGAYAMA T., OHSHIMA I., MURATA R., "Finite element simulation of oblique cutting", *Bulletin of the Japan Society of Precision*, pp. 221-222, 1990.

[MAR 95] MARUSICH T. D., ORTIZ M., "Modeling and simulation of high-speed machining", *Inter. J. for Numerical Methods in Engineering*, pp. 3675-3694, 1995.

[MON76] MONTGOMERY R. S., "Friction and wear at high sliding speeds", *Wear*, pp. 275-298, 1976.

[OBI 97] OBIKAWA T., SASAHARA H., SHIRAKASHI T., USUI E., "Application of computational machining method to discontinuous chip formation", *J. of Manufacturing Sc.*, And Eng., pp. 667-674, 1997.

[PAN 96] PANTALE O., Modélisation et simulation tridimensionnelles de la coupe des métaux, Thesis of Bordeaux University, France, 1996.

[RAK 93] RAKOTOMALALA R., JOYOT P., TOURATIER M., "Arbitrary Lagrangian-Eulerian thermomechanical finite element model of material cutting", *Communications in Numerical Methods in Eng.*, pp. 975-987, 1993.

[SAS 94] SASAHARA H., OBIKAWA T., SHIRAKASHI T., "FEM analysis on 3D cutting", *Inter. J. Japan Soc. Pro. Eng.*, pp. 123-128, 1994.

[SEK 92] SEKHON G. S., CHENOT J. L., "Some simulation experiments in orthogonal cutting", *Numerical methods in Industrial Forming Processes*, pp. 901-906, 1992.

[SEK 93] SEKHON G. S., CHENOT J. L., "Numerical simulation of continuous chip formation during non-steady orthogonal cutting", *Engineering computations*, pp. 31-48, 1993.

[SHI 90] SHIH A. J. M., CHANDRASEKAR S., YANG H. T. Y., "Finite element simulation of metal cutting process with strain-rate and temperature effects", *Fundamental issues in machining ASME*, pp. 11-24, 1990.

[STR 85] STRENKOWSKI J. S., CARROLL J. T., "A finite element model of orthogonal metal cutting", *Winter annual meeting of the ASME*, pp. 157-166, 1985.

[UED 93] UEDA K., MANABE K., "Rigid-plastic FEM analysis of 3D deformation field in chip formation process", *Annals of the CIRP*, pp. 35-28, 1993.